JOURNAL OF VIROLOGY, Apr. 2002, p. 3471–3481 Vol. 76, No. 7
0022-538X/02/$04.00+0 DOI: 10.1128/JVI.76.7.3471–3481.2002

Evidence of a Role for Nonmuscle Myosin II in Herpes Simplex Virus Type 1 Egress

Hans van Leeuwen, Gill Elliott, and Peter O'Hare*

Marie Curie Research Institute, The Chart, Oxted, Surrey RH8 0TL, United Kingdom

Received 1 November 2001/Accepted 7 January 2002

After cell entry, herpes simplex virus (HSV) particles are transported through the host cell cytoplasm to nuclear pores. Following replication, newly synthesized virus particles are transported back to the cell periphery via a complex pathway including a cytoplasmic phase involving some form of unenveloped particle. These various transport processes are likely to make use of one or more components of the cellular cytoskeletal systems and associated motor proteins. Here we report that the HSV type 1 (HSV-1) major tegument protein, VP22, interacts with the actin-associated motor protein nonmuscle myosin IIA (NMIIA). HSV-1 infection resulted in reorganization of NMIIA, inducing retraction of NMIIA from the cell periphery and condensation into a spoke-like distribution around the nucleus along with a second effect of accumulation in a perinuclear cluster. VP22 did not appear to colocalize with the reorganized cagelike distribution of NMIIA. However, VP22 has been previously reported to localize in a perinuclear vesicular pattern, and significant overlap was observed between this pattern and the perinuclear clusters of NMIIA. Inhibition of the ATPase activity of NMIIA with the myosin-specific inhibitor butanedione monoxime impaired the formation of the perinuclear vesicular VP22 accumulations and also the release of virus into the extracellular medium while having much less effect on the yield of cell-associated virus. Virus infection frequently results in the induction of highly extended processes emanating from the infected cell, and we observed that VP22-containing particles line up along NMIIA-containing filaments which run through these protrusions.

The lytic life cycle of herpesviruses involves cell adsorption, fusion and penetration, capsid transport within the host cytoplasm to the nucleus, viral DNA replication, synthesis of viral components, and subsequent virus assembly followed by cytoplasmic transport to the cell periphery and finally release from the cell. Among the first viral proteins encountering the host cell after infection are those of the tegument, a proteinaceous layer assembled between the viral capsid and envelope and comprising at least 12 virus-encoded proteins (18). Following fusion of the virus envelope with the cell membrane, these tegument proteins are immediately involved in a variety of activities which promote virus infectivity, including, for example, shutoff of host protein synthesis (14, 21, 42) or the induction of transcription of the incoming genome in the nucleus (3, 37, 41). There is limited information on the precise fate of the tegument proteins after entry and the nature of their association with the infecting capsid. Based on electron microscopy images of herpes simplex virus type 1 (HSV-1) particles during cell entry, it was suggested that the capsid loses part of its associated tegument proteins, which remain at the cytoplasmic surface of the cell membrane (46). Recent reports indicate that certain tegument proteins are released into the cytoplasm of the infected cells (32) while a subset remains associated with the capsid. It has been proposed that this latter class of tegument proteins may be involved in intracytoplasmic capsid trafficking and docking of capsids to the nuclear pores (2, 38, 46).

Virus particles, particularly in vivo, are unlikely to rely on simple passive diffusion for transportation through the cytoplasm. Early studies using drugs capable of disrupting components of the cellular cytoskeleton indicated involvement of at least some of these networks in herpes simplex virus transport. For example, nocodazole, which causes depolymerization of the microtubule (MT) network, and taxol, which stabilizes MTs, have been reported to inhibit transport of virus particles within neuronal cells (25, 49). More recent work using immunoelectron microscopy of infected cultured neurons has also indicated a role for the MT network (19, 30, 39). However, in nonneuronal cells, drugs which affect the MT network showed little significant inhibition of virus replication (25), suggesting that while MTs may be important for neuronal transport, additional transport mechanisms may be used in nonneuronal cells. Consistent with this, in Vero cells, addition of nocodazole or taxol from 4 h onwards had little affect on virion release (1).

Despite the early results showing the lack of an effect of MT disruption on infectivity (25), cytosolic capsid particles have been observed in association with microtubules in nonneuronal cells early during entry (46). Accumulation of virus particles at the microtubule organizing center, together with the observation of dynein, a minus-end-directed MT-dependent motor protein attached to capsid-tegument structures after entry, lead to the proposal that the MT network and associated motor proteins may be involved in virus transport to the cell nucleus (46, 51). Whatever the precise mechanism(s) of transport, it is likely that structural components of the capsid and tegument will be important for any specific interaction with cellular transport systems. In this regard there have been few published reports documenting specific interactions between viral and cellular components, although it was recently reported that the HSV-1 UL34 gene product interacts with dynein (51). Since it was also shown that UL34 interacts with the

* Corresponding author. Mailing address: Marie Curie Research Institute, The Chart, Oxted, Surrey RH8 0TL, United Kingdom. Phone: 44 1883 722306. Fax: 44 1883 714375. E-mail: p.ohare@mcri.ac.uk.

major capsid protein, ICP5, it was proposed that UL34 could link the capsid to the dynein motor. However, whether this will prove to be relevant for entry remains to be determined, since other workers have demonstrated that at least in pseudorabies, UL34 is not assembled into the mature virion (23).

In this study we set out to identify cellular proteins which interact with the HSV-1 tegument protein, VP22, encoded by the UL49 gene and representing one of the major tegument proteins, present in approximately 1,500 to 2,000 molecules per virion (26). To date the precise role(s) of VP22 in the HSV-1 infection cycle remains unclear. Although VP22 is conserved within the alpha-herpesvirus family, it has been reported that the intact VP22 protein, at least, is not necessary for virus replication (40). Whether VP22 is completely dispensable for HSV replication remains to be established. In addition, VP22 may have more than a structural role, since the protein was shown to exhibit unusual intracellular properties which could be involved in some distinct aspect of replication, independent of assembly (12). Here we show that VP22 interacts with nonmuscle myosin IIA (NMIIA), a motor protein which is recruited to the actin cytoskeleton and has been reported to be involved in numerous dynamic cellular processes, including Golgi budding, vesicle secretion, cell spreading, cleavage and migration, and cell adhesion (for a review, see reference 43). We show that HSV-1 infection induces the retraction of NMIIA from the cell periphery and its accumulation in a spoke-like pattern around the nucleus. NMIIA also accumulates in a perinuclear cluster, colocalizing with VP22 in sites proposed to be viral assembly compartments. We also observed that HSV infection frequently induces the formation of long protrusions from the cell, and using a recombinant virus expressing VP22 fused to the green fluorescent protein (GFP-VP22), we found that GFP-VP22-containing punctate structures frequently align along myosin filaments within these protrusions. Finally, blocking myosin ATPase activity significantly reduces the yield of extracellular virus while having little effect on cell-associated virus. Based on these observations, we speculate that myosin may play a role in virus transport during HSV replication.

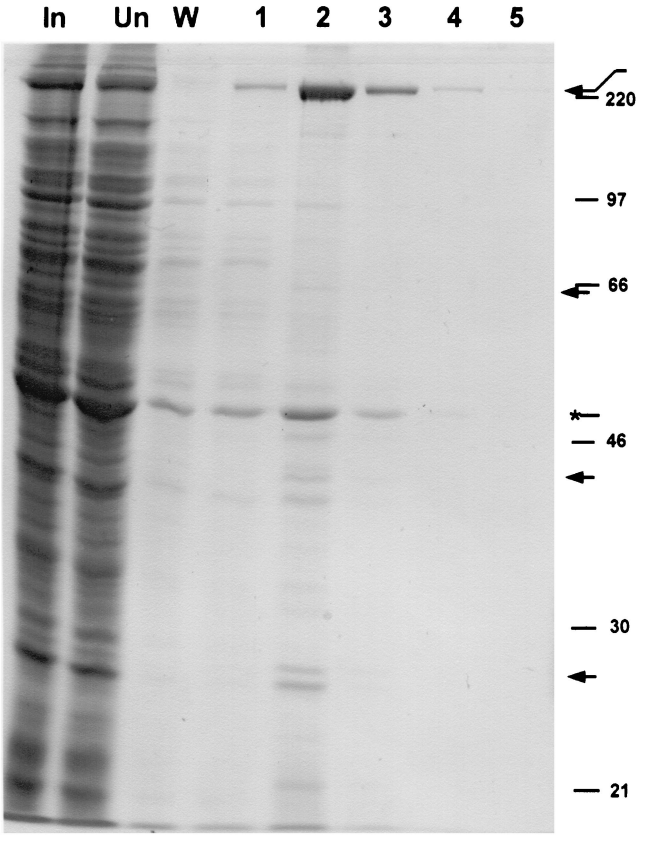

FIG. 1. Affinity purification of VP22-associated proteins from infected BHK cell extracts. Purified antibody to GST-VP22 was covalently coupled to an affinity support. A soluble extract of HSV-1-infected BHK cells (10^9 cell equivalents) was clarified and precleared over a control column. This input material (In) was then passed over the anti-VP22 column, the unbound material was collected (Un), and the column was washed in buffer (W). Bound material was then eluted in several fractions in a low-pH buffer (numbered fractions 1 to 5). Equal cell equivalents of each of the samples were then analyzed by SDS-PAGE and total protein staining. Arrows indicate the positions of bands that were selectively retained on the column. Migration of molecular size markers is indicated on the right side in kilodaltons. The asterisk indicates the position of a band migrating at approximately 47 kDa

MATERIALS AND METHODS

Cell culture, transfections, and infections. Vero cells and BHK cells were maintained in Dulbecco's modified minimal essential medium containing 10% newborn calf serum. Cells were transfected with plasmid DNA using the calcium phosphate precipitation method with BES [*N*,*N*-bis(2-hydroxyl)-2-aminoethanesulfonic acid]-buffered saline, as previously described (17). Cells were processed for immunofluorescence approximately 40 h after transfection. Virus infections were carried out with HSV-1 strain 17 or HSV-1 strain 166 expressing GFP-VP22 as previously described (13). For examination of protein synthesis in the absence and presence of butanedione monoxime (BDM), cells were infected (multiplicity of infection [MOI] of 10), and after incubation for 1 h, the medium was replaced with medium containing various concentrations of BDM and the cells were maintained in this medium. One hour before harvesting, labeling medium containing the same concentrations of BDM and supplemented with [^{35}S]methionine (20 μC/ml) was added, and incubation continued for 1 h. The cells were then washed in phosphate-buffered saline (PBS) and harvested in sodium dodecyl sulfate (SDS) lysis buffer. For immunoprecipitation the cells were lysed in RIPA buffer and clarified by centrifugation at 10,000 × *g* for 20 min, and extracts were incubated with the anti-VP22 specific antibody AGV30 (1:150). After separation by SDS-polyacrylamide gel electrophoresis (PAGE), protein synthesis was assessed by autoradiography.

Immunofluorescence. Vero cells grown on glass coverslips (either transfected or infected) were washed twice with PBS and fixed in 4% paraformaldehyde in PBS at room temperature for 10 min. The fixed cells were permeabilized by 10 min of treatment with 0.5% Triton X-100 followed by three 5-min washes with PBS. The cells were then blocked in PBS containing 10% calf serum for 10 min at room temperature. Primary antibodies were added in the same solution and incubated for 45 min at room temperature. Following two 5-min washes with PBS, secondary antibodies were added in blocking buffer and incubated for 15 min. After an additional two washes in PBS, the coverslips were mounted in Mowiol (Sigma) containing 2.5% 1,4-diazabicyclo-2.2.2-octane to reduce bleaching. Samples were examined by confocal microscopy using a Zeiss LSM410 confocal microscope, and images were annotated using Adobe Photoshop software. Immunofluorescence of cells with phalloidin-stabilized cytoskeleton was performed as described previously (48).

Plasmids. The VP22 expression vector pAP85H contains the VP22 open reading frame under the control of the human cytomegalovirus immediate-early promoter and has been described previously (8).

Antibodies and reagents. Antibodies used in this study and their dilutions for immunofluorescence were as follows: polyclonal antibody against bacterially expressed and purified VP22, AGV30 (1:500); monoclonal antibody to the hemagglutinin epitope (1:200) and monoclonal myosin heavy chain (1:100), obtained from Babco (Richmond, Va.); antibodies against nonmuscle myosin II (1:600), kindly provided by J. Kendrick-Jones; butanedione monoxime, used at concen-

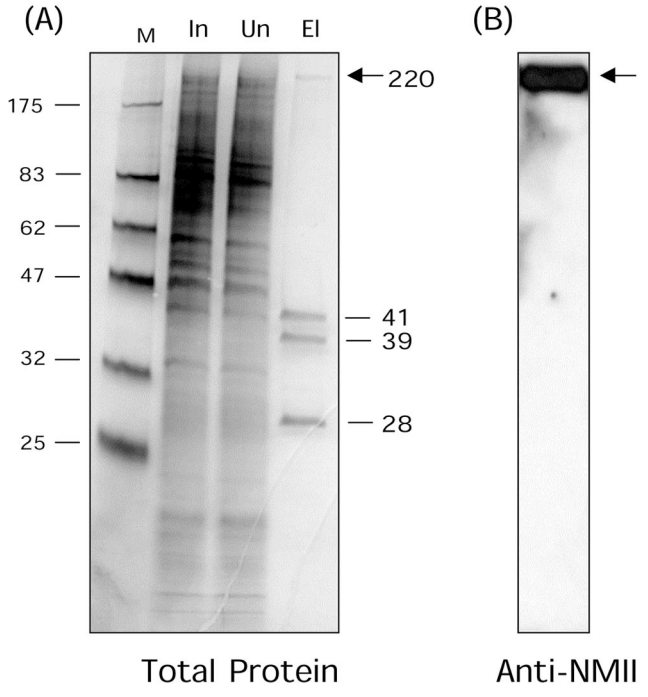

FIG. 2. Direct affinity purification of VP22-associated proteins from uninfected HeLa cell extracts. (A) Cell extracts (2×10^{10} cells) were passed over a VP22 affinity column, constructed as described in Materials and Methods. Lanes: M, molecular size standard; In, input (2×10^4 cell equivalents); Un, unbound (2×10^4 cell equivalents); El, 600 mM NaCl elution fraction (10^8 cell equivalents). Proteins were separated by SDS-PAGE and detected by silver staining. While the vast majority of proteins were not retained on the column, a high degree of enrichment of four species was observed (numbers indicate molecular mass in kilodaltons). (B) The elution fraction was transferred to nitrocellulose and reacted with anti-nonmuscle myosin II antibody. Elution fraction arrows indicate a large species of approximately 225 kDa in the bound fraction eluting at 600 mM NaCl.

trations ranging from 5 to 40 mM, and phalloidin, obtained from Sigma-Aldrich (Dorset, England).

VP22 affinity chromatography. Purification of VP22-associated proteins was performed in two ways. In the first approach, VP22-associated proteins were purified from HSV-1-infected cells on an anti-VP22 antibody column. In the second approach, VP22 itself was overexpressed in bacteria, purified, and coupled to a solid support. Uninfected cell proteins were then chromatographed on the VP22 column.

1) Purification of VP22-associated proteins from infected cells. Monolayers of BHK cells were infected with HSV-1 strain 17, (MOI 0.1), and after >80% cytopathic effect was observed, a soluble extract was prepared by extraction in a high-salt buffer consisting of 400 mM NaCl, 20 mM HEPES (pH 7.9), 1 mM EDTA, 5% (vol/vol) glycerol, 1 mM dithiothreitol, plus the following cocktail of protease inhibitors: 1 mM phenylmethylsulfonyl fluoride (PMSF), 0.22 mM *N*α-*p*-tosyl-L-lysine chloromethyl ketone, 2 μg of leupeptin/ml, 2 μg of aprotinin/ml, and 1 μg of pepstatin A/ml. The extracts were clarified by centrifugation at 10,000 × *g* for 20 min at 4°C. Antibody to VP22, prepared by immunization with a highly purified glutathione *S*-transferase (GST)-VP22 fusion protein (12), was purified on protein A-Sepharose beads, eluted, and then covalently coupled to activated CnBr-Sepharose beads as described by the manufacturer (Pharmacia). The soluble infected cell extracts were first diluted to 200 mM NaCl, precleared over control Protein A-Sepharose beads, and finally incubated with the anti-VP22 antibody column for 2 h at 4°C. Unbound material was collected, the column was washed in 0.1 M Tris-HCl, and bound proteins were then eluted in 0.1 M glycine (pH 3.2). Fractions were analyzed by SDS-PAGE, electroblotted onto polyvinyl difluoride membranes, bands were excised and trypsin digested, and peptides were fractionated by high-performance liquid chromatography (HPLC) and microsequenced.

2) Purification of VP22 binding proteins by direct interaction. We first expressed and purified VP22 protein in bacteria. Numerous attempts to express the intact protein have been unsuccessful, but expression and purification of the core conserved domain of VP22 has been achieved. The construction of the prokaryotic expression vector (pVP24) for the bacterial expression of the conserved core domain of VP22, amino acids 159 to 301 (VP22.C1) linked to an N-terminal His tag, has been described previously (34). VP22.C1 was purified by Ni^{2+}-nitrilotriacetic acid (NTA) column chromatography exactly as described previously (34) with the inclusion of an additional step of cation exchange chromatography on a Mono S HR 5/5 column (Pharmacia). Using a linear gradient of increasing salt concentration, VP22.C1 eluted at approximately 400 mM NaCl and was purified as a homogeneous single band (>98% pure). The purified protein (4 mg) was then rebound to a 2-ml NTA column for the subsequent purification of VP22 binding species. To that end, HeLa cells (approximately 2×10^{10}) were suspended in 100 ml of lysis buffer containing 50 mM Tris (pH 8.0), 150 mM NaCl, 1% Nonidet P-40, 0.5 mM (PMSF), and Complete protease inhibitor cocktail according to the instructions of the manufacturer (Boehringer Mannheim). After incubation for 45 min on ice with occasional mixing, the lysate was diluted 1:1 in buffer containing 50 mM Tris (pH 7.0), 50 mM NaCl, and 0.5 mM PMSF. Insoluble material was removed by centrifugation (30 min, 12,000 rpm). Before being applied to the VP22 affinity column, clarified lysates were loaded onto a 15-ml NTA column equilibrated in wash buffer containing 50 mM Tris (pH 7.5), 100 mM NaCl, 0.1% NP-40, and 0.5 mM PMSF to remove nonspecific binding proteins. The unbound flowthrough from this column was adjusted to 20 mM imidazole (pH 7.0) and 150 mM NaCl and loaded onto the VP22-NTA column equilibrated in buffer A (50 mM Tris [pH 7.0], 10% glycerol, 0.1% NP-40, 100 mM NaCl, 2.5 mM β-mercaptoethanol, Complete protease inhibitor). After extensive washing in buffer A, specifically bound proteins were eluted with a 30-ml linear gradient of 100 to 1,000 mM NaCl. Eluted fractions were analyzed by SDS-PAGE and silver staining. For protein identification, isolated bands were excised after SDS-PAGE and subjected to trypsin digestion, reverse-phase HPLC separation of the peptides, and microsequencing. Unambiguous sequence was obtained and screened against protein databases.

RESULTS

HSV-1 major tegument protein VP22 binds NMIIA. To investigate aspects of the function of the HSV tegument protein VP22, we wished to identify cellular proteins with which the protein may interact, and we pursued two approaches to that end. We first made an anti-VP22 antibody affinity column in order to isolate VP22-associated proteins from HSV-infected cells. The antibody was produced in rabbits against a bacterially expressed GST-VP22 fusion protein that had been purified by glutathione affinity chromatography. The antibody, which reacted against a single band in Western blotting of infected cell extracts (13), was purified by protein A-Sepharose chromatography and then covalently coupled to CnBr-activated Sepharose. Soluble extracts of HSV-1-infected BHK cells (10^9 cell equivalents), prepared as described in Materials and Methods, were precleared over a control column and then passed over the anti-VP22 antibody column. Unbound material was collected, the column was washed, and bound material was eluted with a low-pH buffer. The input material and unbound and eluted fractions were then analyzed by SDS-PAGE and total protein staining (Fig. 1).

While the majority of proteins were found in the unbound fraction (Fig. 1), several bands peaking in the elute fraction 2 were highly enriched on the anti-VP22 antibody column. Note that several species in the eluted fractions appeared to represent the trailing off of nonspecifically bound proteins which had not been completely removed from the column and were seen in the wash fraction (Fig. 2). Nevertheless, clear enrichment of several proteins was observed. Among the prominent bands, the bands migrating at approximately 38 and 65 kDa likely represent VP22 and VP16, and indeed we have previ-

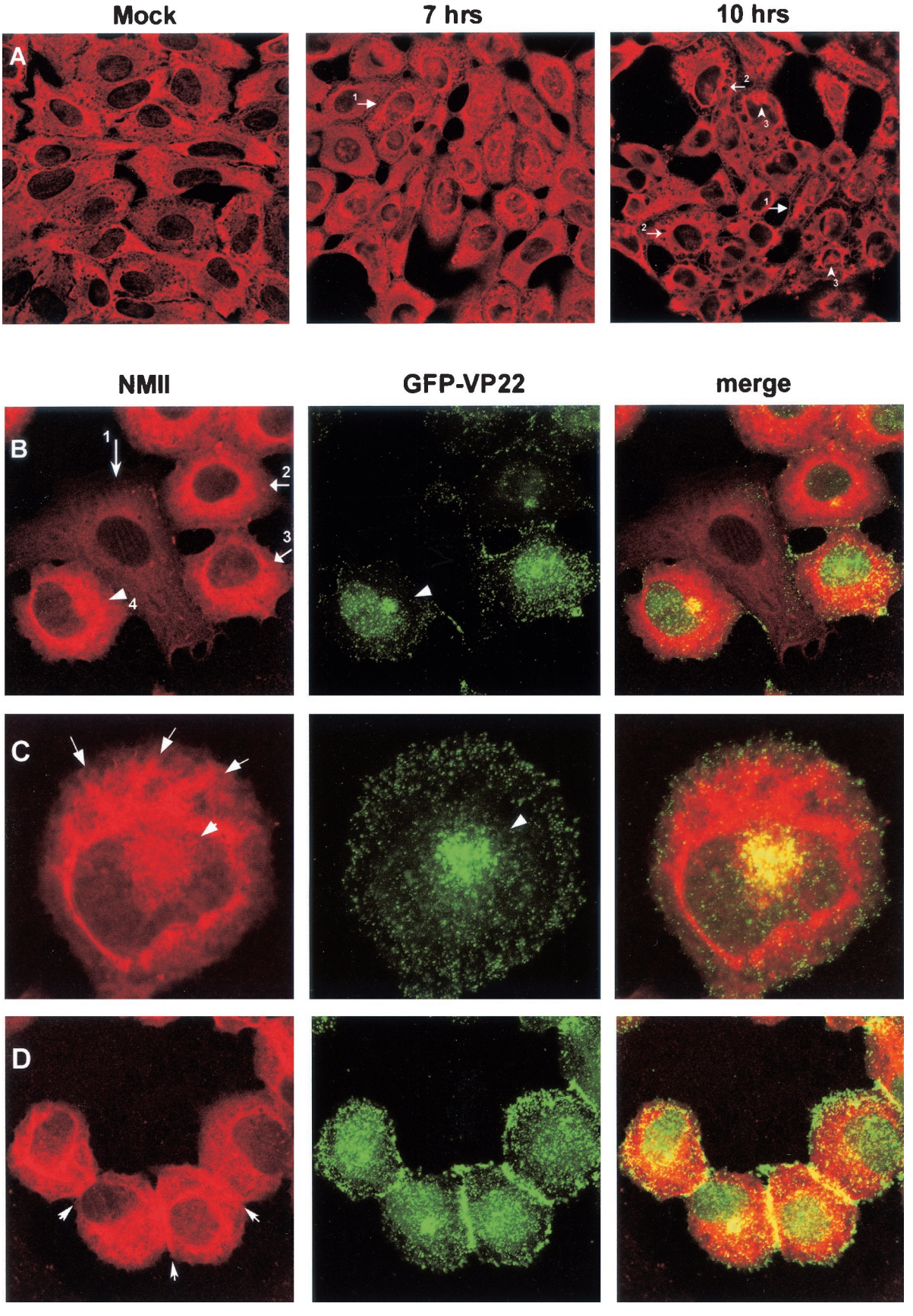
Mock
7 hrs
10 hrs
A
1
2
3
1
2
3
NMII
GFP-VP22
merge
B
1
2
3
4
C
D

ously shown that VP22 copurifies with VP16 in immunoprecipitation experiments using anti-VP16 monoclonal antibody (10). The band migrating at approximately 47 kDa is likely to be actin (Fig. 1), but its appearance in the wash fraction may indicate that this represents nonspecific binding of a relatively abundant cell species (but see below). The most prominent species retained on the column, migrating at approximately 225 kDa, did not appear in the wash fraction and was highly enriched. This was the only protein obtained in sufficient amounts to facilitate identification by amino acid sequencing. The fraction was transferred to a polyvinylidene difluoride membrane, the 225-kDa species was isolated from the blot and trypsin digested, and the peptides were purified by HPLC. Sequencing of several peptides followed by database searching identified a perfect match to rat (and human) myosin heavy chain, which it is reasonable to assume would be identical to the sequence of the hamster homologue (not yet in the database), considering that the extracts were made from infected baby hamster kidney cells. Myosin heavy chain has a predicted size of 225 kDa, consistent with the migration of the purified band.

Several considerations make it unlikely that the purification of myosin heavy chain was due to a nonspecific interaction. First, the extract was precleared, and myosin heavy chain was not observed to bind to control Sepharose columns. Second, the anti-VP22 antibody was made against highly purified GST-VP22 that was purified from bacteria, which do not contain myosin. Third, the anti-VP22 antibody was highly specific and showed no cross-reaction to other species, e.g., on Western blots of infected cell lysates (13). Nevertheless, in parallel we pursued an alternative approach to the identification of VP22-associated species, by the overexpression and purification of VP22 itself, and the chromatography of, in this case, uninfected cell extracts on a VP22 affinity column.

Numerous attempts to express intact VP22 in bacteria were unsuccessful, but expression and purification of the core conserved domain of VP22 has been achieved as described previously (34). VP22.C1 (amino acids 159 to 301 containing an N-terminal His tag) was purified by Ni^{2+}-NTA column chromatography as described in Materials and Methods, and the purified protein (>98% pure) was recoupled to a fresh NTA column. Soluble extracts of HeLa cells (2×10^{10} cells), first precleared over uncoupled NTA columns to remove nonspecific NTA-binding proteins, were then passed over the VP22 column. Unbound material was collected, the column was washed extensively, and bound proteins were then eluted by increasing salt concentration (Fig. 2A). The majority of proteins in the input sample (In) were not retained on the column, with the flowthrough sample (Un) appearing virtually identical to the load (Fig. 2A). However we observed selective binding and a high degree of enrichment of four cellular proteins, including a large species of approximately 225 kDa in the bound fraction eluting at 600 mM NaCl (Fig. 2A). Each of these proteins was purified for identification by microsequencing of HPLC-purified peptides, obtained after trypsin digestion of the isolated bands. (None of the proteins was retained on the control columns used for preclearing the extracts). Two proteins (Fig. 2A, 41 and 39 kDa) were identified as template activating factor Ia and Ib (33), involved in nucleosome assembly and in microtubule dynamics, possibly through association with cyclins (22). The smallest VP22-associated protein (Fig. 2A, 28 kDa), was identified as mapmodulin, which has been reported to enhance transport of Golgi vesicles in a microtubule- and dynein-dependent manner (50). It is possible that these species were also bound in the first approach on the antibody column, but in that case insufficient quantities were obtained for sequencing, and their identification will await development of specific antibodies. The possible role of binding of VP22 to these proteins is currently under investigation and will be pursued elsewhere.

With respect to the identity of the large 225-kDa VP22-associated protein, a database search of an amino acid sequence obtained from this band (KVSHLLGINVTDFTRG) showed that it unequivocally corresponded to the amino acid sequence present in the human protein NMIIA (45). NMIIA is one of the two vertebrate nonmuscle myosin heavy chains (the other being NMIIB) and is expressed, with a few exceptions, in most cell types (43). NMIIA has a predicted molecular weight of 225 kDa, consistent with the migration of the VP22 binding protein. The identity of the protein was further pursued by Western blotting of the VP22 bound protein fraction with a polyclonal antibody specific for nonmuscle myosin II species (kindly supplied by John Kendrick-Jones), showing a single 225-kDa reactive band (Fig. 2B). There are no reports of the additional proteins identified above interacting with myosin, and together with the data from the independent approach on the antibody column, our results provide strong evidence for a direct interaction between VP22 and NMIIA. It remains formally possible that the NMIIA-VP22 association is indirect, via NMIIA interaction with one of the other bound species.

NMIIA has been reported to be involved in a number of cellular processes, including Golgi budding, vesicle secretion, cell spreading, cleavage, and migration (7, 20, 29). In view of the possibility that tegument proteins make reasonable candidates for involvement in transport of virus particles within cells, the observation of a motor protein, associated with a cytoskeletal network, binding specifically to a VP22 affinity column was intriguing. We therefore undertook a series of

FIG. 3. Alterations in nonmuscle myosin II localization patterns in infected cells. (A) Nonmuscle myosin II retracts from the cell edge during virus infection. Mock-infected (Mock) or HSV-1-infected Vero cells were fixed and stained with antibody against nonmuscle myosin II at 7 and 10 h p.i. as indicated. Nonmuscle myosin II staining was reduced at the cell periphery (no. 1 arrows) and was accompanied by condensation into a spoke-like pattern (no. 2 arrows) and frequent perinuclear clustering (no. 3 arrows). (B to D) Alterations in nonmuscle myosin II localization patterns in infected cells. Vero cells were infected with HSV-1 166v which expressed GFP-VP22, fixed, and stained, and the distribution of anti-myosin II (red) or GFP-VP22 (green) was examined. Merged images are shown in the right panel. Arrowheads in panel B indicate perinuclear clusters. Arrow no. 1 indicates a cell not yet expressing GFP-VP22, in which NMIIA exhibits the more typical cytoplasmic staining; arrows 2 to 4 indicate cells expressing GFP-VP22, in which NMIIA staining has become more intense. Arrows in panel C indicate the condensed spoke-like pattern of nonmuscle myosin II in infected cells. Arrows in panel D indicate accumulation of NMIIA at cell-cell junctions. Several features of the alteration in nonmuscle myosin II and GFP-VP22 are shown in each of the panels as discussed in the text.

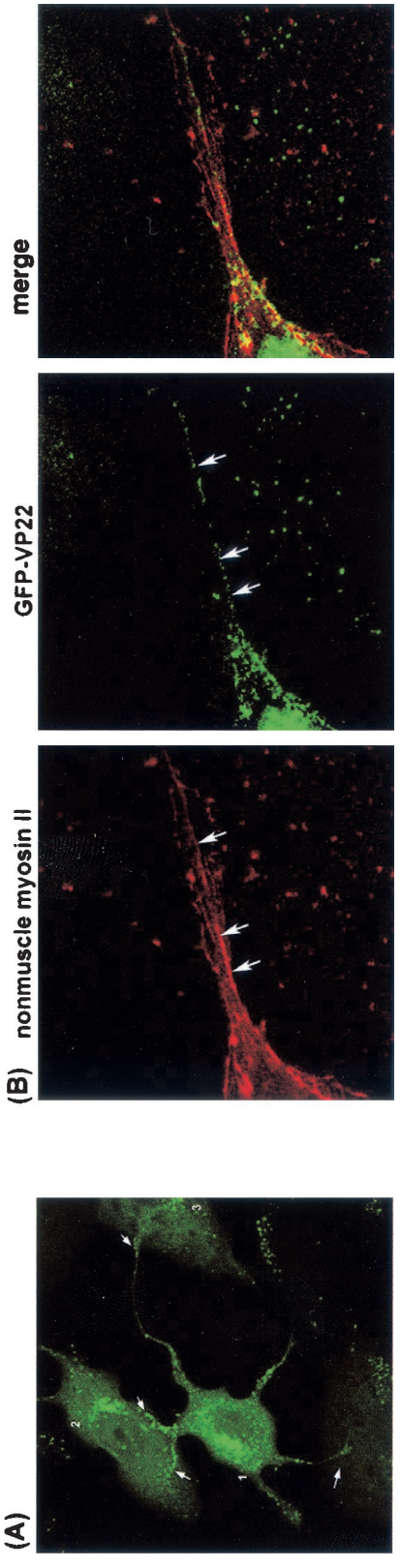

FIG. 4. HSV-induced cell protrusions. (A) Typical example of a Vero cell infected with HSV-1 166v where highly extended protrusions containing GFP-VP22 vesicles can be seen extending to and making intimate contact with adjacent cells. Arrows indicate the membrane extensions coming from one cell (cell no. 1). (B) A high-magnification image of a section of an infected cell containing protrusions and stained for nonmuscle myosin II. Filaments containing NMIIA can be detected running through the protrusions (arrows, left panel). GFP-VP22-containing particles (arrows, center panel) align along nonmuscle myosin II filaments within the protrusions.

experiments to further examine the interaction between NMIIA and VP22. (Note that the antibody employed in the studies below does not discriminate between NMIIA and NMIIB, but for the sake of simplicity we have indicated the target protein as NMIIA.)

We first attempted to establish any colocalization between the two components in Vero cells transfected with a VP22 expression vector and stained for NMIIA and VP22. NMIIA exhibited a dispersed cytoplasmic staining frequently showing a mesh-like pattern, together with localization in close proximity to the plasma membrane (Fig. 3A). In transfected cells, VP22 appears mostly in a diffuse cytoplasmic pattern (11). This diffuse pattern showed some, but incomplete, colocalization with NMIIA (data not shown). Generally, notwithstanding the results showing a biochemical association between the two proteins, it was difficult from the transfection experiments to draw a conclusion that the overlap in diffuse heterogeneous localization reflected a direct interaction.

Multiple effects of HSV-1 infection on NMIIA distribution. We therefore next examined NMIIA localization in HSV-1 infected cells. Vero cells infected with HSV-1 (MOI of 10) or mock infected were fixed at different times after infection and stained for NMIIA (Fig. 3). Several significant alterations in the appearance of NMIIA were observed in the infected cells. While NMIIA normally exhibited cytoplasmic staining with significant accumulation at the cell periphery, (Fig. 3A, Mock), in infected cells NMIIA appeared to retract from the cell edges (Fig. 3, 10 h, no. 1 arrows). Concomitant with this, NMIIA appeared to concentrate in a distinct spoke-like pattern more around the nucleus (Fig. 3A, 10 h, and 3C). NMIIA also accumulated in a perinuclear cluster which was more readily observed when the cluster appeared over the nucleus (Fig. 3A, 10 h, and 3C). These effects on myosin were observed between 5 and 7 h after infection and were pronounced by 10 h after infection (Fig. 3A).

To examine further NMIIA and VP22 localization, we next made use of a recombinant HSV-1 strain, 166v, containing the VP22 gene fused to the GFP gene, facilitating visualization of particles and compartments containing VP22 (13). Parallel examination of VP22 by GFP fluorescence and of NMIIA by immunofluorescence revealed several points, as illustrated in Fig. 3B to D. Thus, as previously described, we observed a pronounced concentration of VP22 in small punctate vesicular structures throughout the cell, with frequent perinuclear clusters (Fig. 3B, GFP-VP22). These perinuclear clusters have been proposed to be possible sites of incorporation of VP22 into assembling virions (13). The alteration in the appearance of NMIIA during infection can be seen by comparing a cell not yet expressing GFP-VP22 (Fig. 3B, NMIIA, arrow 1) in which NMIIA exhibits the more typical cytoplasmic staining, with cells expressing GFP-VP22 in which NMIIA staining has become more intense, with pronounced condensation around the nucleus (Fig. 3B). However, we did not note any distinct colocalization with the condensed spoke-like pattern of NMIIA and GFP-VP22. Conversely, where we observed a distinct perinuclear cluster of GFP-VP22, significant colocalization with a subpopulation of NMIIA could be observed (Fig. 3B, GFP-VP22 arrowhead, NMIIA no. 4 arrow). The alteration in NMIIA and its relationship with VP22 localization can be more clearly seen in the higher-magnification image of an

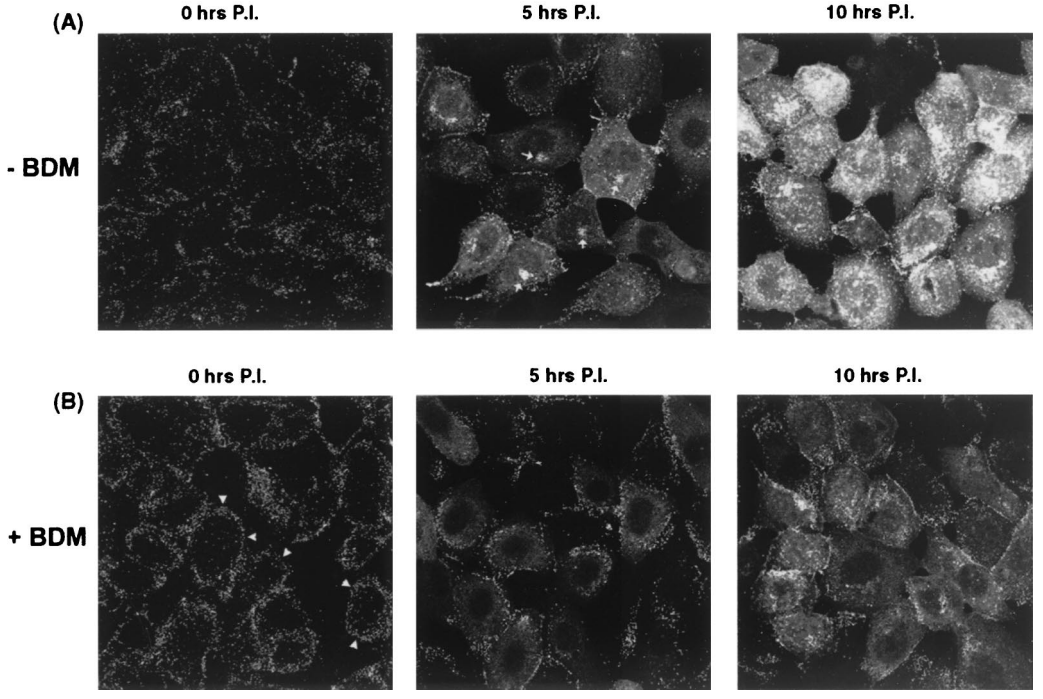

FIG. 5. BDM inhibits formation of perinuclear virus assembly complexes. Vero cells were incubated in the absence (A) or presence (B) of 10 mM BDM and then infected with HSV-1 166v (MOI 50). Cells were then fixed immediately or 5 or 10 h p.i. as indicated, and the pattern of intrinsic fluorescence of GFP-VP22 was examined. BDM induced the retention of input material at the cell periphery, as indicated by arrowheads in panel B (0 h). The perinuclear accumulation of GFP-VP22 observed during the normal time course of infection (indicated by arrows in panel A, 5 h) was significantly reduced in the presence of BDM.

infected cell (Fig. 3C). The spoke-like pattern of NMIIA which was usually observed together with concentration encircling the nucleus can be clearly seen, but with no obvious colocalization with VP22. GFP-VP22 clustering to one side of the nucleus (and in this image lying over the nucleus), exhibited significant colocalization and overlap with NMIIA clustering (Fig. 3C, GFP-VP22, NMIIA, and merged image). NMIIA typically appeared to encompass the GFP-VP22 clusters. An additional feature of NMIIA localization in infected cells is shown in Fig. 3D. In these cells, abundant particulate GFP-VP22 material could be observed accumulating at the cell-cell contacts (Fig. 3D, GFP-VP22), possibly reflecting cell-to-cell spread of virus particles (see Discussion). Interestingly, distinct accumulation of NMIIA also occurred at these junctions (Fig. 3D), appearing yellow in the merged image. Since myosins are proposed to be involved in organelle transport, the colocalization of GFP-VP22-containing compartments with a population of NMIIA may reflect a role of NMIIA in transport of virus compartments or particles during virus egress.

We noted during the course of our analysis using HSV 166v the frequent observation that in live infected cells, extended processes could be readily observed extending from the plasma membrane and penetrating into adjacent cells. Such extensions are thin and could extend up to several cell lengths, and they were not readily observed in conventional immunofluorescence studies, probably due to their fragility during fixation conditions. A typical example of this is shown in Fig. 4A, where several protrusions are seen extending from one cell to make contact with adjacent cells. Note that the punctate GFP-VP22 material indicated by the thin arrows over cells labeled 2 and 3 actually originate from cell 1. Fluorescent GFP-VP22-containing spots could be observed progressing along these extensions and accumulating at the extremities contacting the adjacent cells. From this and additional time-lapse microscopy, it appears that the formation of these extensions is not a simple consequence of a cytopathic effect. Rather, we believe their formation, and the accumulation of GFP-VP22-containing vesicles within them, is an active process likely to be relevant to cell-to-cell spread of the virus. Since formation of cellular extensions is a process which is known to involve the actin/myosin system, we wished to examine any association between NMIIA and VP22 in these structures.

Cells were treated with phalloidin just prior to fixation in order to stabilize the actin cytoskeleton and were examined at high magnification for the distribution of NMIIA and GFP-VP22. Filaments containing NMIIA could be detected running through the protrusions (Fig. 4B, left panel). Within the protrusions there was a significant degree of association with GFP-VP22 foci along these filaments (Fig. 4B, right panel). Outside the protrusions themselves, as indicated above, colocalization was not seen throughout the cytoplasm, being restricted to the perinuclear clustering described above (Fig. 3). But within the extensions, GFP-VP22 foci were frequently observed in tracks, and these tracks represented filaments containing NMIIA.

The GFP-VP22-containing fluorescent spots could represent some form of intermediate in virus assembly: vesicles containing intermediates or secretory vesicles containing enveloped virions in transit to the periphery of the extension.

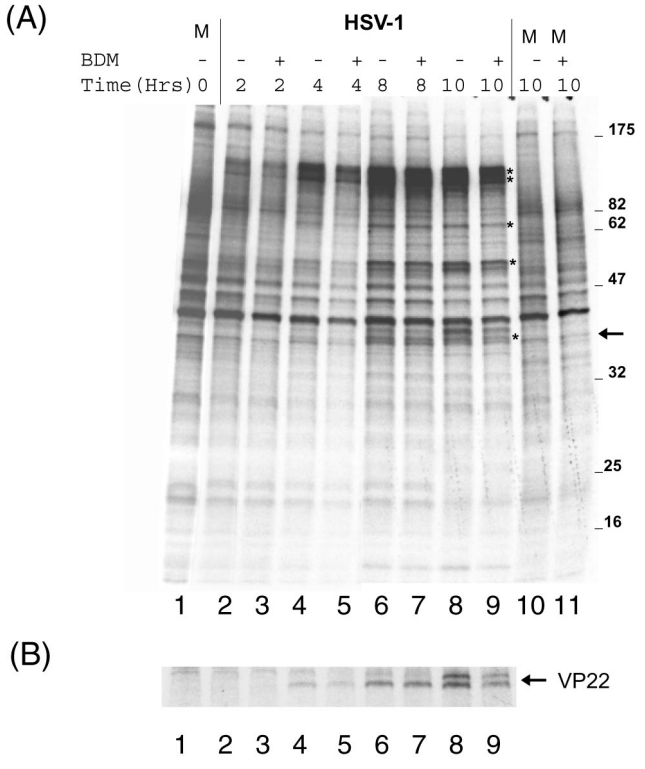

FIG. 6. BDM has no significant effect on ongoing virus protein synthesis. (A) Vero cells were mock infected (M) or infected with HSV-1 (MOI of 10), and after 1 h ($t = 0$), medium was replaced with medium containing no BDM (−) or 10 mM BDM (+). Labeling medium containing ^{35}S-methionine (including BDM where appropriate) was added to cells at the indicated times, and incubation continued for 1 h. Cells were then harvested and analyzed by SDS-PAGE and autoradiography. Asterisks indicate the position of major infected cell-specific proteins. (B) As for panel A, except that the cells were extracted in RIPA buffer and VP22 was immunoprecipitated using a specific polyclonal antibody. The two bands represent differentially phosphorylated forms of VP22.

Blocking myosin ATPase activity inhibits perinuclear accumulation of GFP-VP22 clusters. To provide additional evidence on the possible involvement of myosin in virus assembly or transport, we made use of the cell-permeable drug BDM. While it is not specific to the NMIIA class, BDM is the most selective myosin inhibitor available and effectively inhibits myosin activity by slowing the release of phosphate from the myosin head after ATP hydrolysis (7). Vero cells were infected with HSV-1 (166v), and localization of GFP-VP22 was examined in living cells at various times after infection in the presence and absence of BDM (10 mM). Immediately after infection (Fig. 5, 0 h), punctate cell surface material representing the total inoculum was observed. This material had largely disappeared by 5 h, by which time de novo synthesized GFP-VP22 was now seen in a diffuse cytoplasmic pattern, together with commencement of perinuclear vesicular clustering as described above (Fig. 5A). By 10 h postinfection (p.i.), intense fluorescent perinuclear distribution was observed together with abundant punctate and vesicular accumulation throughout the cytoplasm. In contrast, in the presence of BDM, we found that progression of infection was retarded, and several changes were observed compared to the control infections (Fig. 5B). Immediately after infection, a pronounced effect was observed in that the input fluorescent inoculum was present in a more obviously peripheral distribution (Fig. 5B, 0 h). In the presence of BDM, this peripheral material was maintained longer than in the absence of BDM (Fig. 5B, 5 h). Furthermore, while diffuse cytoplasmic GFP-VP22 was observed, no prominent perinuclear vesicular accumulation was observed (compare Fig. 5, − BDM and + BDM, 5 and 10 h). Since the diffuse cytoplasmic VP22 pattern reflects newly synthesized protein rather then incoming virus-associated VP22 (12), BDM did not appear to affect entry of that population of infectious virions which results in the progressive protein synthesis. To confirm this, we examined infected cell protein synthesis under identical conditions. Infected or mock-infected cells were incubated in the presence of BDM (10 mM) and pulse labeled with ^{35}S-methionine for 1 h before harvest. Total protein synthesis was then assessed after SDS-PAGE of the cell lysates and autoradiography (Fig. 6A), while expression of VP22 was assessed by immunoprecipitation (Fig. 6B). Neither the kinetics nor the accumulation of herpesvirus proteins, including VP22, was significantly affected by the presence of BDM (Fig. 6A and B, compare − BDM and + BDM at each time point). Thus, despite the accumulation of fluorescent material at the cell periphery in the presence of BDM, our results suggest that entry and release of the viral genomes into the nucleus, at least as judged by subsequent virus protein synthesis, were not significantly affected by the drug (see Discussion).

Furthermore, while there was only a minor effect on levels of virus protein synthesis, recruitment and formation of VP22 in vesicular perinuclear compartments were significantly retarded by BDM.

Effect of blocking myosin ATPase on release of virus particles. From the immunofluorescence studies above, NMIIA appeared to form a cluster around perinuclear sites containing GFP-VP22, which may be associated with virus assembly, and BDM, an inhibitor of myosin activity, retarded the vesicular accumulation of GFP-VP22. These results suggested the possible involvement in virus assembly or egress. To gain additional evidence for this possibility, we examined the effects of inhibiting myosin at late stages of infection on the production of extracellular and cell-associated virus. Although BDM appeared to have little gross cytopathic effect over the time course of the experiments described above, we wished to minimize any effect of the inhibitor on the cells per se. Therefore, in examining the effect of BDM on the production of infectious virus, the inhibitor was added to cells at 12 h p.i., and virus yield was assayed 8 h later, at 20 h p.i. Vero cells (10^6 cells) were infected with HSV-1 (MOI of 10), and at 12 h after infection, BDM was added at a range of concentrations. Incubation was continued for a further 8 h, after which time the extracellular medium was collected and the yield of virus was determined (Fig. 7). The results show that addition of BDM at a 10 mM concentration inhibited the release of infectious virus by approximately 20-fold. Higher concentrations of BDM did not block release more efficiently. The reduction in virus release typically ranged from 20- to 50-fold, and while moderate compared to, e.g., inhibition by acycloguanosine, the effect of BDM was greater than any previously observed with inhibitors

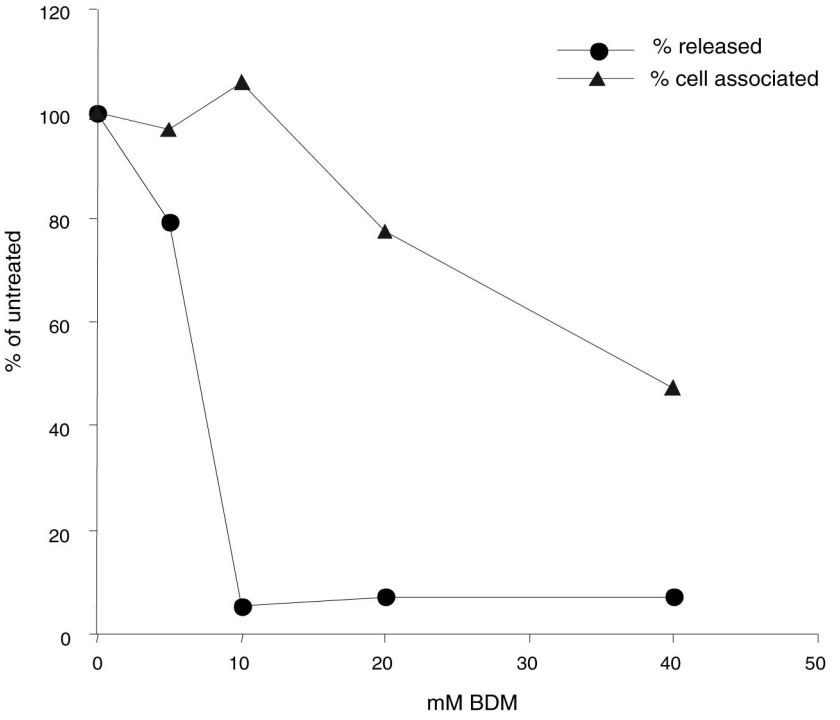

FIG. 7. Effect of BDM on the yield of infectious virus. Monolayers of Vero cells (10^6) were infected with HSV-1 strain 17 (MOI of 10), and BDM was added at a range of concentrations at 12 h p.i. At 20 h p.i., medium (circles) or cell-associated virus (triangles) was collected, and the numbers of released was viruses determined by plaque assay. Results are plotted as a percentage of the yields of virus in the absence of drug, which were 1.1×10^5 for released virus and 0.5×10^5 for cell-associated virus.

which act upon cytoskeletal organization. In parallel measurements, at doses which had a significant effect on the production of extracellular virus, BDM had very little effect on the yield of cell-associated virus (Fig. 7). In addition, no morphological cytopathic effect was observed (data not shown), nor, as shown above, was there any significant effect on virus or cellular protein synthesis (Fig. 6). These results indicate that the effect of BDM on production of extracellular virus was a specific one.

DISCUSSION

Replication of HSV at the cellular level requires vectoral transport of particles within the cytoplasm to and from the nucleus. At a different but related level, one main aspect of pathogenesis in humans involves vectoral transport of virus from the site of infection along axons to the sensory neurons which harbor latent virus and conversely from these neurons back to the periphery. Initial examination of intracellular transport mechanisms involved in virus assembly or egress largely revolved around ultrastructural analysis and the effect of drugs such as nocodazole, Taxol, or cytochalasins on virus release (25, 28, 36, 49). More recent studies have included more refined immunoelectron-microscopic analysis within neurons in culture and examination of capsids interacting specifically with the microtubule network (19, 30, 46), but the detailed mechanisms involved in vectoral transport of HSV remain poorly understood. For example, with one exception (see below), there have been no reports of HSV structural proteins interacting specifically with the motor proteins or other transport components which would be candidate targets for movement on the cytoskeletal networks. The data to date suggest an involvement of the microtubule network in virus transport. Here we report several lines of evidence which indicate that the HSV-1 major tegument protein, VP22, associates with NMIIA, an actin-associated motor protein, and that this interaction may be relevant for virus transport or egress. We first used affinity chromatography to identify cellular VP22 binding proteins within soluble extracts of HeLa cells and observed a high degree of enrichment and selective binding of four proteins, including NMIIA. While the relevance of the additional VP22-associated proteins is currently under investigation, there are no reports of these proteins interacting with myosin, and we believe that the VP22-myosin association is a direct one. Tegument proteins clearly represent strong candidates as viral proteins which may be involved in interactions with cellular transport systems.

We next analyzed NMIIA in infected cells by using a GFP-VP22-expressing HSV-1 strain to examine VP22 colocalization. We observed that NMIIA retracted from the cell edges as infection progressed and accumulated frequently in a spoke-like fashion in the cytoplasm of infected cells. Alterations in the microtubule network (1) and intermediate filament networks (35) have been previously reported. In addition, previous work has indicated that actin-containing microfilaments are reorganized during HSV infection (4, 36). While it may not be surprising that NMIIA localization is altered, we also observed a population of NMIIA which colocalized with GFP-VP22 in and surrounding perinuclear clusters which we previ-

ously proposed to be associated with the Golgi apparatus and to represent compartments relevant to the virus assembly pathway (13). Furthermore late in infection we observed accumulation of GFP-VP22-containing particles at the junctions between adjacent cells, likely reflecting aspects of cell-to-cell spread of assembled virus, and here too distinct colocalization with NMIIA could be observed.

Additional evidence for a role of myosin in virus replication was obtained using the drug BDM, which inhibits the ATPase activity of myosins. BDM added at a relatively late stage of infection (12 h), when viral protein synthesis and DNA replication were well under way, resulted in a significant reduction in virus release. Interestingly, BDM added at the initiation of infection did not severely inhibit entry of infectious virus (as judged by subsequent levels of protein synthesis), but subsequent formation of the distinct perinuclear assembly structures was significantly reduced. We believe that the inhibition of myosin affects recruitment and formation of the perinuclear clusters and that this results in reduction or retardation of the release of infectious virus.

We noted that despite the lack of an effect on early de novo protein synthesis, addition of BDM at the beginning of infection nevertheless resulted in the peripheral retention of GFP-VP22-containing particles immediately after infection. This material normally began to disappear immediately after infection and was largely lost from the surface by 4 to 5 h after infection. An explanation consistent with the BDM-induced peripheral retention of input material could be related to the known inhibition of myosin-dependent endocytosis by BDM (9, 15). Thus, if a population of input material, possibly that population not infectious by the normal route of fusion, was taken up by endocytosis, then addition of BDM may prevent or retard the endocytic fate of such material. Since the normal physiologically relevant route of HSV entry does not rely on endocytosis for cell entry, this would be consistent with the absence of a significant effect on de novo protein synthesis. Further work with purified virions should help clarify this point and whether these observations are related, e.g., to estimation of particle/PFU ratios.

The family of myosins currently comprises at least 16 classes of motor proteins, and it is becoming increasingly clear that many members of the myosin family play a role(s) in the transport of intracellular organelles and vesicles (43). Nonmuscle myosin II appears to be the only member of the myosin super-family with the ability to form polymeric molecular assemblies (6). In conjunction with filamentous actin, it plays a role in cell shape changes during the cell cycle, division, and spreading (29). Although myosin II has not yet been reported to be involved in long-range vesicular transport, additional roles that have been reported for NMIIA include receptor capping, driving neurite outgrowth, neurotransmitter release at synaptic membranes (31), and budding of trans-Golgi transport vesicles (20), although this latter role is debated (44). NMIIA also takes part in the assembly of a network of actin filaments supporting the plasma membrane of eukaryotic cells, the actin cortex (16, 27, 47). At cell junctions, rapid structural reorganizations of the actin cytoskeleton results in expansion of the intercellular contact and the formation of myosin II arcs at boundaries, indicating a role for this protein in the formation of such junctions (16, 24). Thus, currently the VP22-myosin interaction could be relevant at any of a number of different stages of assembly and egress, and further work will be necessary to identify the role of the interaction in detail. However, we believe the results provide evidence for an interaction with a network other than the microtubule/dynein system.

Furthermore, we found that infected cells frequently form very pronounced plasma membrane protrusions which establish intimate contact with adjacent cells. This behavior was not a passive effect of a virus-induced cytopathic effect but an active process induced by infection that may be relevant for cell-to-cell spread. While further characterization of these events is under way, we observed that GFP-VP22-containing particles line up in these protrusions with actin-based myosin II filaments. It is possible that the punctate GFP-VP22-containing foci may represent intermediates in assembly, wherein nonmuscle myosin II present on actin cables could bind directly to VP22. It is conceivable that some features of transport within induced extensions in culture may reflect certain aspects of the specialized transport in vivo, and further work is under way to examine this.

In summary, our observations on the interaction between a herpesvirus tegument protein and an actin-based myosin motor protein together with the effects of BDM suggest that the myosin-actin network could play a role in virus transport. Previous proposals that transport of virus particles may occur on microtubules (30, 46) do not exclude actin from participating in transport. An accepted concept is that long-range movement of vesicles occurs on microtubules and short-range movement occurs on actin filaments, with actin filaments bridging the gaps and arranging the local delivery. For example, nerve ends contain few MTs, and synaptic vesicles are thought to travel on actin cables at the periphery, beyond the reach of MTs (5). Further experiments are now under way on examination of the VP22-myosin interaction combined with, e.g., real-time visualization of transport in GFP-VP22-infected cells and neurons after addition of myosin inhibitors to clarify the role of the actin-myosin network in virus assembly and/or transport.

ACKNOWLEDGMENTS

We thank John Kendrick Jones for provision of nonmuscle myosin II antibody. We also thank Anne Phelan and Alison Whiteley for discussion and advice.

This work was supported by a long-term EMBO fellowship to H.V.L. and Marie Curie Cancer Care.

REFERENCES

1. **Avitabile, E., S. Di Gaeta, M. R. Torrisi, P. L. Ward, B. Roizman, and G. Campadelli-Fiume.** 1995. Redistribution of microtubules and Golgi apparatus in herpes simplex virus-infected cells and their role in viral exocytosis. J. Virol. **69:**7472–7482.
2. **Batterson, W., D. Furlong, and B. Roizman.** 1983. Molecular genetics of herpes simplex virus. VIII. Further characterization of a temperature-sensitive mutant defective in release of viral DNA and in other stages of the viral reproductive cycle. J. Virol. **45:**397–407.
3. **Batterson, W., and B. Roizman.** 1983. Characterization of the herpes simplex virion-associated factor responsible for the induction of alpha genes. J. Virol. **46:**371–377.
4. **Bedows, E., K. M. Rao, and M. J. Welsh.** 1983. Fate of microfilaments in vero cells infected with measles virus and herpes simplex virus type 1. Mol. Cell. Biol. **3:**712–719.
5. **Brown, S. S.** 1999. Cooperation between microtubule- and actin-based motor proteins. Annu. Rev. Cell Dev. Biol. **15:**63–80.
6. **Cheney, R. E., M. A. Riley, and M. S. Mooseker.** 1993. Phylogenetic analysis of the myosin superfamily. Cell Motil. Cytoskelet. **24:**215–223.

7. **Cramer, L. P., and T. J. Mitchison.** 1995. Myosin is involved in postmitotic cell spreading. J. Cell Biol. **131:**179–189.
8. **Dilber, M. S., A. Phelan, A. Aints, A. J. Mohamed, G. Elliott, C. I. Edvard Smith, and P. O'Hare.** 1999. Intercellular delivery of thymidine kinase prodrug activating enzyme by the herpes simplex virus protein, VP22. Gene Ther. **6:**12–21.
9. **Durrbach, A., K. Collins, P. Matsudaira, D. Louvard, and E. Coudrier.** 1996. Brush border myosin-I truncated in the motor domain impairs the distribution and the function of endocytic compartments in an hepatoma cell line. Proc. Natl. Acad. Sci. USA **93:**7053–7058.
10. **Elliott, G., G. Mouzakitis, and P. O'Hare.** 1995. VP16 interacts via its activation domain with VP22, a tegument protein of herpes simplex virus, and is relocated to a novel macromolecular assembly in coexpressing cells. J. Virol. **69:**7932–7941.
11. **Elliott, G., and P. O'Hare.** 2000. Cytoplasm-to-nucleus translocation of a herpesvirus tegument protein during cell division. J. Virol. **74:**2131–2141.
12. **Elliott, G., and P. O'Hare.** 1997. Intercellular trafficking and protein delivery by a herpesvirus structural protein. Cell **88:**223–233.
13. **Elliott, G., and P. O'Hare.** 1999. Live-cell analysis of a green fluorescent protein-tagged herpes simplex virus infection. J. Virol. **73:**4110–4119.
14. **Fenwick, M. L., and S. A. Owen.** 1988. On the control of immediate early (alpha) mRNA survival in cells infected with herpes simplex virus. J. Gen. Virol. **69:**2869–2877.
15. **Geli, M. I., and H. Riezman.** 1996. Role of type I myosins in receptor-mediated endocytosis in yeast. Science **272:**533–535.
16. **Gloushankova, N. A., N. A. Alieva, M. F. Krendel, E. M. Bonder, H. H. Feder, J. M. Vasiliev, and I. M. Gelfand.** 1997. Cell-cell contact changes the dynamics of lamellar activity in nontransformed epitheliocytes but not in their ras-transformed descendants. Proc. Natl. Acad. Sci. USA **94:**879–883.
17. **Greaves, R., and P. O'Hare.** 1989. Separation of requirements for protein-DNA complex assembly from those for functional activity in the herpes simplex virus regulatory protein Vmw65. J. Virol. **63:**1641–1650.
18. **Haarr, L., and S. Skulstad.** 1994. The herpes simplex virus type 1 particle: structure and molecular functions. Review article. APMIS **102:**321–346.
19. **Holland, D. J., M. Miranda-Saksena, R. A. Boadle, P. Armati, and A. L. Cunningham.** 1999. Anterograde transport of herpes simplex virus proteins in axons of peripheral human fetal neurons: an immunoelectron microscopy study. J. Virol. **73:**8503–8511.
20. **Ikonen, E., J. B. de Almeid, K. F. Fath, D. R. Burgess, K. Ashman, K. Simons, and J. L. Stow.** 1997. Myosin II is associated with Golgi membranes: identification of p200 as nonmuscle myosin II on Golgi-derived vesicles. J. Cell Sci. **110:**2155–2164.
21. **Jones, F. E., C. A. Smibert, and J. R. Smiley.** 1995. Mutational analysis of the herpes simplex virus virion host shutoff protein: evidence that vhs functions in the absence of other viral proteins. J. Virol. **69:**4863–4871.
22. **Kellogg, D. R., and A. W. Murray.** 1995. NAP1 acts with Clb1 to perform mitotic functions and to suppress polar bud growth in budding yeast. J. Cell Biol. **130:**675–685.
23. **Klupp, B. G., H. Granzow, and T. C. Mettenleiter.** 2000. Primary envelopment of pseudorabies virus at the nuclear membrane requires the UL34 gene product. J. Virol. **74:**10063–10073.
24. **Krendel, M. F., and E. M. Bonder.** 1999. Analysis of actin filament bundle dynamics during contact formation in live epithelial cells. Cell Motil. Cytoskelet. **43:**296–309.
25. **Kristensson, K., E. Lycke, M. Roytta, B. Svennerholm, and A. Vahlne.** 1986. Neuritic transport of herpes simplex virus in rat sensory neurons in vitro. Effects of substances interacting with microtubular function and axonal flow [nocodazole, taxol and erythro-9–3-(2-hydroxynonyl)adenine]. J. Gen. Virol. **67:**2023–2028.
26. **Leslie, J., F. J. Rixon, and J. McLauchlan.** 1996. Overexpression of the herpes simpex virus type 1 tegument protein VP22 increases its incorporation into virus particles. Virology **220:**60–68.
27. **Li, D., M. Miller, and P. D. Chantler.** 1994. Association of a cellular myosin II with anionic phospholipids and the neuronal plasma membrane. Proc. Natl. Acad. Sci. USA **91:**853–857.
28. **Lycke, E., B. Hamark, M. Johansson, A. Krotochwil, J. Lycke, and B. Svennerholm.** 1988. Herpes simplex virus infection of the human sensory neuron. An electron microscopy study. Arch. Virol. **101:**87–104.
29. **Maciver, S. K.** 1996. Myosin II function in non-muscle cells. Bioessays **18:**179–182.
30. **Miranda-Saksena, M., P. Armati, R. A. Boadle, D. J. Holland, and A. L. Cunningham.** 2000. Anterograde transport of herpes simplex virus type 1 in cultured, dissociated human and rat dorsal root ganglion neurons. J. Virol. **74:**1827–1839.
31. **Mochida, S., H. Kobayashi, Y. Matsuda, Y. Yuda, K. Muramoto, and Y. Nonomura.** 1994. Myosin II is involved in transmitter release at synapses formed between rat sympathetic neurons in culture. Neuron **13:**1131–1142.
32. **Morrison, E. E., A. J. Stevenson, Y. F. Wang, and D. M. Meredith.** 1998. Differences in the intracellular localization and fate of herpes simplex virus tegument proteins early in the infection of Vero cells. J. Gen. Virol. **79:**2517–2528.
33. **Nagata, K., H. Kawase, H. Handa, K. Yano, M. Yamasaki, Y. Ishimi, A. Okuda, A. Kikuchi, and K. Matsumoto.** 1995. Replication factor encoded by a putative oncogene, set, associated with myeloid leukemogenesis. Proc. Natl. Acad. Sci. USA **92:**4279–4283.
34. **Normand, N., H. van Leeuwen, and P. O'Hare.** 2001. Particle formation by the HSV protein VP22 enabling protein and nucleic acid delivery. J. Biol. Chem. **276:**15042–15050.
35. **Norregard Nielsen, L., J. Forchhammer, E. Dabelsteen, A. Jepsen, C. Stubbe Teglbjaerg, and B. Norrild.** 1987. Herpes simplex virus-induced changes of the keratin type intermediate filament in rat epithelial cells. J. Gen. Virol. **68:**737–748.
36. **Norrild, B., V. P. Lehto, and I. Virtanen.** 1986. Organization of cytoskeleton elements during herpes simplex virus type 1 infection of human fibroblasts: an immunofluorescence study. J. Gen. Virol. **67:**97–105.
37. **O'Hare, P.** 1993. The virion transactivator of herpes simplex virus. Semin. Virol. **4:**145–155.
38. **Ojala, P. M., B. Sodeik, M. W. Ebersold, U. Kutay, and A. Helenius.** 2000. Herpes simplex virus type 1 entry into host cells: reconstitution of capsid binding and uncoating at the nuclear pore complex in vitro. Mol. Cell. Biol. **20:**4922–4931.
39. **Penfold, M. E., P. Armati, and A. L. Cunningham.** 1994. Axonal transport of herpes simplex virions to epidermal cells: evidence for a specialized mode of virus transport and assembly. Proc. Natl. Acad. Sci. USA **91:**6529–6533.
40. **Pomeranz, L. E., and J. A. Blaho.** 2000. Assembly of infectious Herpes simplex virus type 1 virions in the absence of full-length VP22. J. Virol. **74:**10041–10054.
41. **Preston, C. M., M. C. Frame, and M. E. Campbell.** 1988. A complex formed between cell components and an HSV structural polypeptide binds to a viral immediate early gene regulatory DNA sequence. Cell **52:**425–434.
42. **Read, G. S., and N. Frenkel.** 1983. Herpes simplex virus mutants defective in the virion-associated shutoff of host polypeptide synthesis and exhibiting abnormal synthesis of alpha (immediate early) viral polypeptides. J. Virol. **46:**498–512.
43. **Sellers, J. R.** 2000. Myosins: a diverse superfamily. Biochim. Biophys. Acta **1496:**3–22.
44. **Simon, J. P., T. H. Shen, I. E. Ivanov, D. Gravotta, T. Morimoto, M. Adesnik, and D. D. Sabatini.** 1998. Coatomer, but not P200/myosin II, is required for the in vitro formation of trans-Golgi network-derived vesicles containing the envelope glycoprotein of vesicular stomatitis virus. Proc. Natl. Acad. Sci. USA **95:**1073–1078.
45. **Simons, M., M. Wang, O. W. McBride, S. Kawamoto, K. Yamakawa, D. Gdula, R. S. Adelstein, and L. Weir.** 1991. Human nonmuscle myosin heavy chains are encoded by two genes located on different chromosomes. Circ. Res. **69:**530–539.
46. **Sodeik, B., M. W. Ebersold, and A. Helenius.** 1997. Microtubule-mediated transport of incoming herpes simplex virus 1 capsids to the nucleus. J. Cell Biol. **136:**1007–1021.
47. **Sullivan, R., L. S. Price, and A. Koffer.** 1999. Rho controls cortical F-actin disassembly in addition to, but independently of, secretion in mast cells. J. Biol. Chem. **274:**38140–38146.
48. **Symons, M. H., and T. J. Mitchison.** 1991. Control of actin polymerization in live and permeabilized fibroblasts. J. Cell Biol. **114:**503–513.
49. **Topp, K. S., L. B. Meade, and J. H. LaVail.** 1994. Microtubule polarity in the peripheral processes of trigeminal ganglion cells: relevance for the retrograde transport of herpes simplex virus. J. Neurosci. **14:**318–325.
50. **Ulitzur, N., M. Humbert, and S. R. Pfeffer.** 1997. Mapmodulin: a possible modulator of the interaction of microtubule-associated proteins with microtubules. Proc. Natl. Acad. Sci. USA **94:**5084–5089.
51. **Ye, G. J., K. T. Vaughan, R. B. Vallee, and B. Roizman.** 2000. The herpes simplex virus 1 U(L)34 protein interacts with a cytoplasmic dynein intermediate chain and targets nuclear membrane. J. Virol. **74:**1355–1363.